

Supplementary Information

**Transition Metal Modification and Carbon Vacancies Promoted Cr<sub>2</sub>CO<sub>2</sub> (MXenes): A New Opportunity for Highly Active Catalyst for Hydrogen Evolution Reaction**

**Yu-Wen Cheng<sup>1</sup>, Jian-Hong Dai<sup>2</sup>, Yu-Min Zhang<sup>1</sup>, Yan Song<sup>2</sup>**

**1** Science and Technology on Advanced Composites in Special Environments Laboratory, Harbin Institute of Technology, Harbin 150001, PR China

**2** School of Materials Science and Engineering, Harbin Institute of Technology at Weihai, 2 West Wenhua Road, Weihai, 264209, PR China

Corresponding author:

E-mail: sy@hitwh.edu.cn; zhym@hit.edu.cn

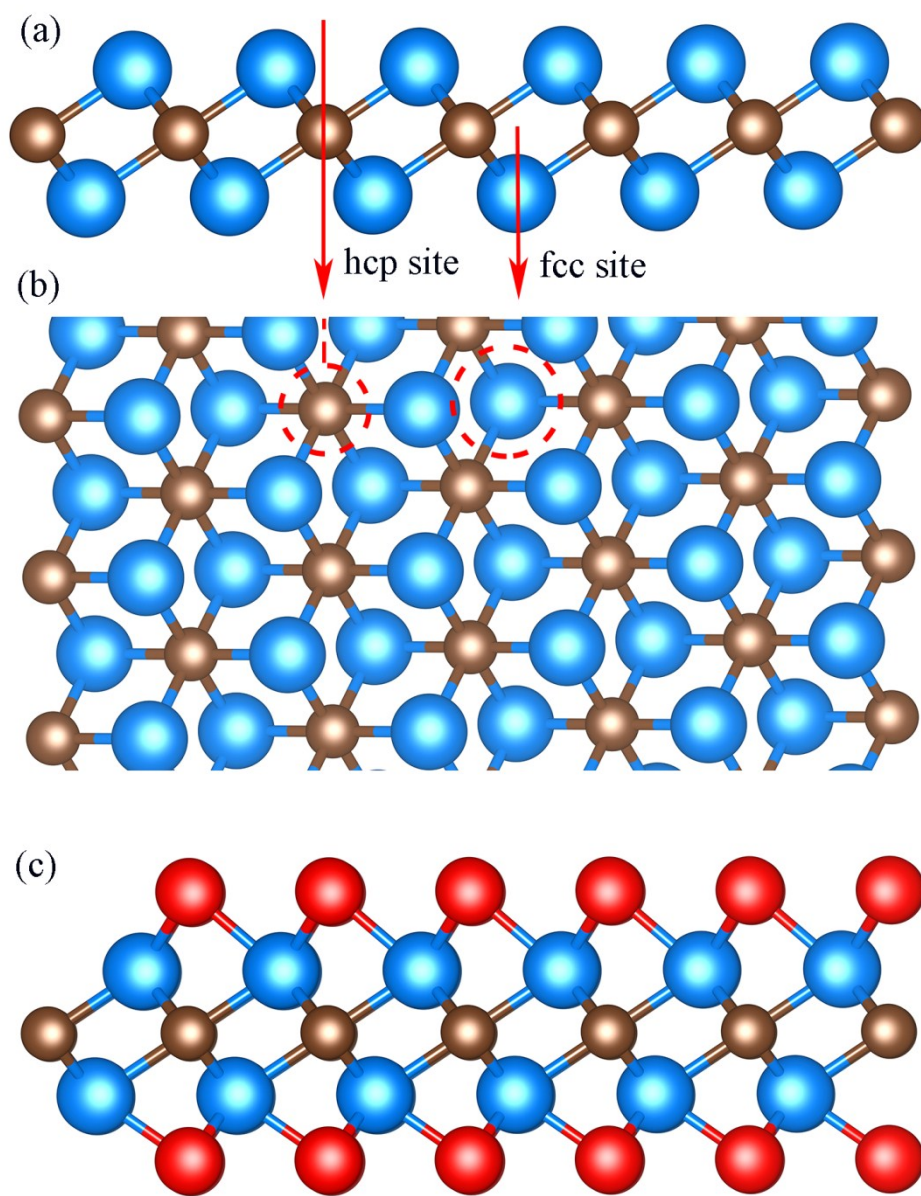


**Figure S1.** Lattice structures of  $\text{Cr}_2\text{C}$  and  $\text{Cr}_2\text{CO}_2$ . (a) side view of  $\text{Cr}_2\text{C}$ , (b) top view of  $\text{Cr}_2\text{C}$ , and (c) side view of  $\text{Cr}_2\text{CO}_2$

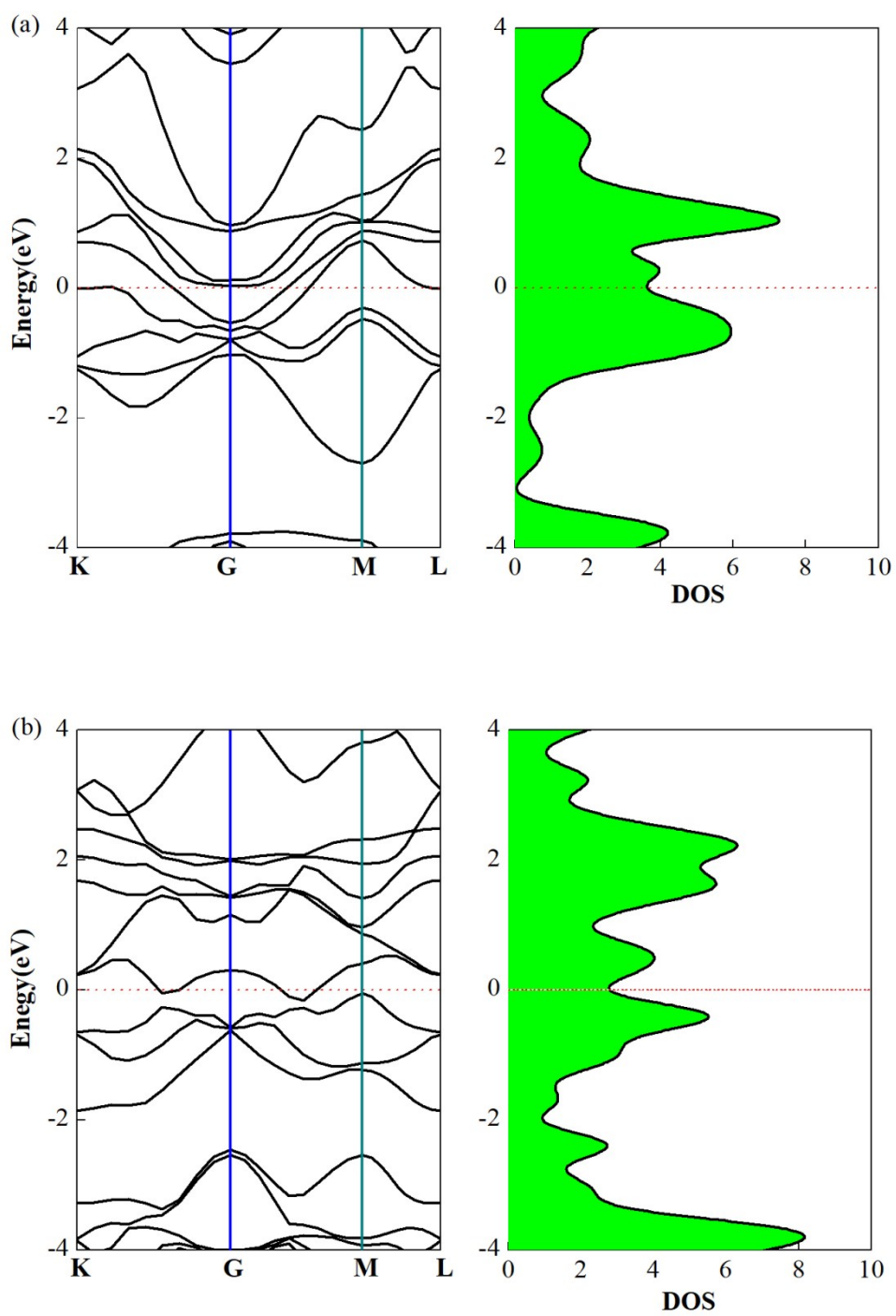


**Figure S2.** Band structure (left) and density of states (right) of (a)  $\text{Cr}_2\text{C}$  and (b)  $\text{Cr}_2\text{CO}_2$ .

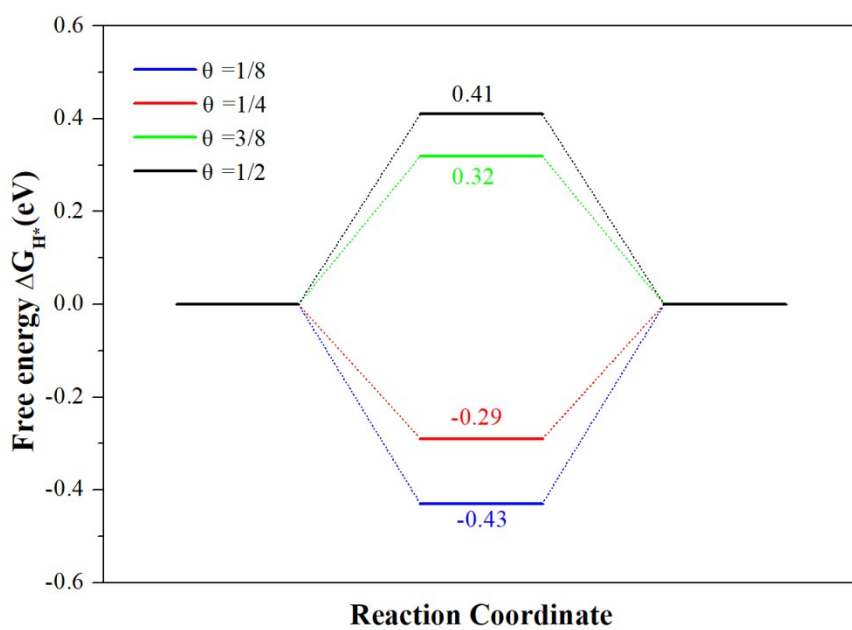


Figure S3. Free energy diagram of HER processing of  $\text{Cr}_2\text{CO}_2$  under different H coverage □.

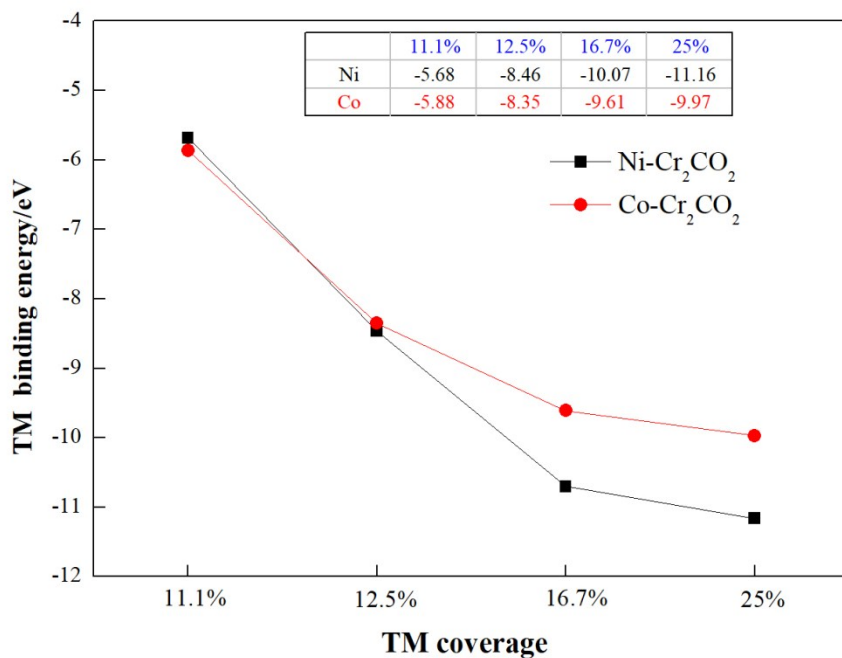
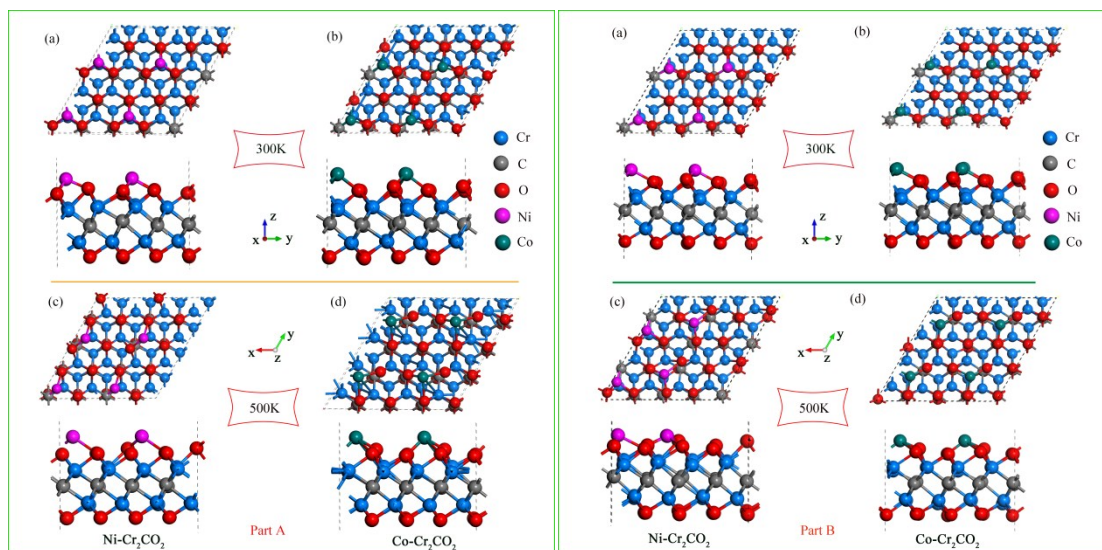
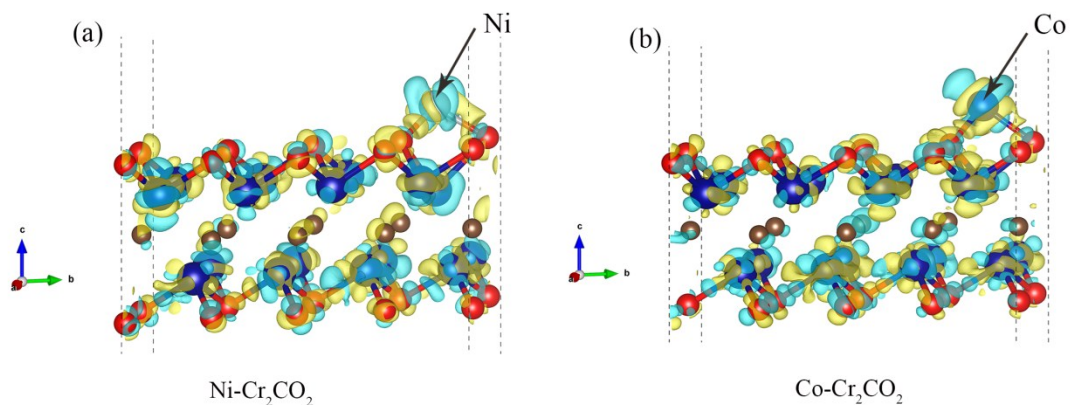


Figure S4. The binding energy of transition metal with  $\text{Cr}_2\text{CO}_2$  surface.



**Figure S5.** Atomic configurations of TM-Cr<sub>2</sub>CO<sub>2</sub> after AIMD simulations under 300K and 500K. The AIMD calculations were typically run for 8ps (Part A) and 4ps (Part B), with a time step of 2 fs.



**Figures S6.** Charge density difference of (a) Ni-Cr<sub>2</sub>CO<sub>2</sub> and (b) Co-Cr<sub>2</sub>CO<sub>2</sub> under 12.5% TM coverage. The light blue and yellow colors denote the negative and positive areas, respectively.

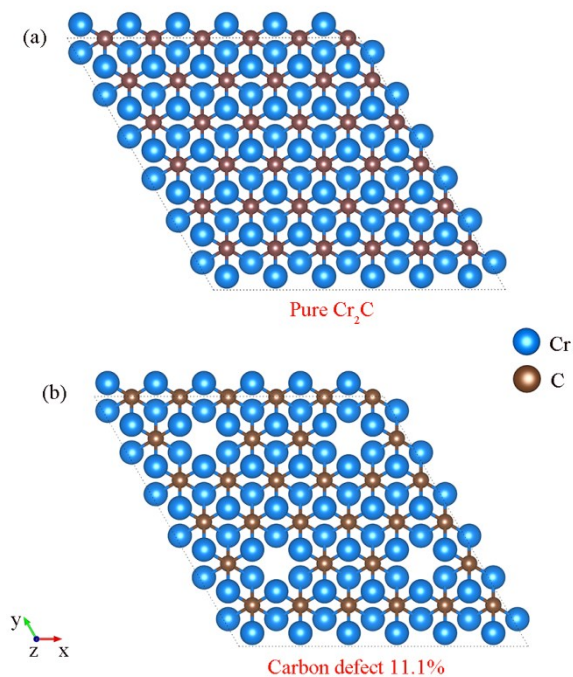


**Figure S7.** The schematics of (a) perfect  $\text{Cr}_2\text{CO}_2$  and (b)  $\text{V}_\text{C}$ - $\text{Cr}_2\text{CO}_2$ . The concentration of carbon vacancies is 11.11%. In this figure we use  $\text{Cr}_2\text{C}$  rather than  $\text{Cr}_2\text{CO}_2$  to identify the carbon vacancies.

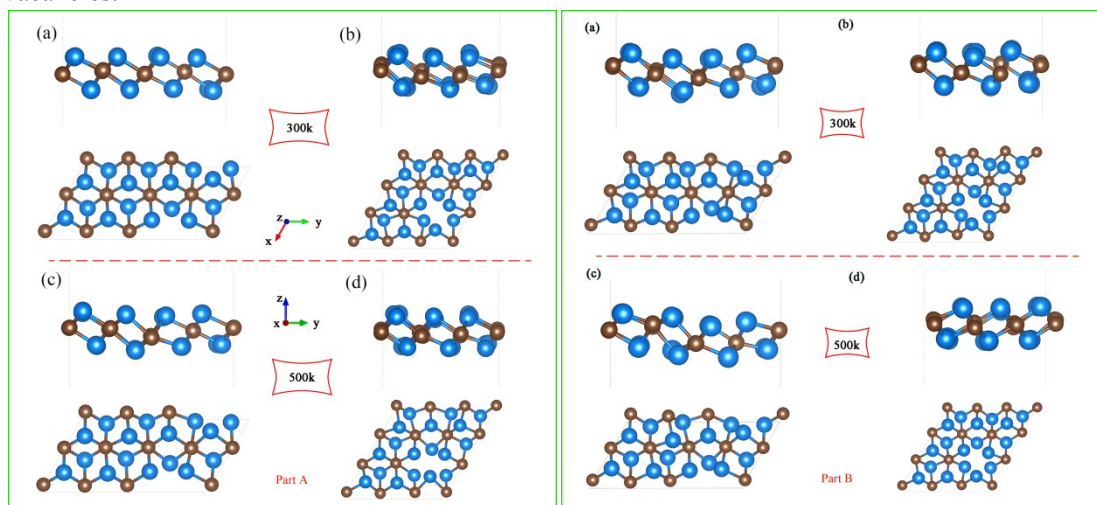


**Figure S8.** Atomic configurations of  $\text{V}_\text{C}$ - $\text{Cr}_2\text{C}$  after *ab initio* molecular dynamics (AIMD) simulations under the temperature of 300K and 500K. The AIMD calculations were typically run for 8ps (Part A) and 4ps (Part B), with a time step of 2 fs. (a) 12.5%  $\text{V}_\text{C}$ - $\text{Cr}_2\text{C}$  at 300K, (b) 11.11%  $\text{V}_\text{C}$ - $\text{Cr}_2\text{C}$  at 300K, (c) 12.5%  $\text{V}_\text{C}$ - $\text{Cr}_2\text{C}$  at 500K, and (d) 11.11%  $\text{V}_\text{C}$ - $\text{Cr}_2\text{C}$  at 500K.

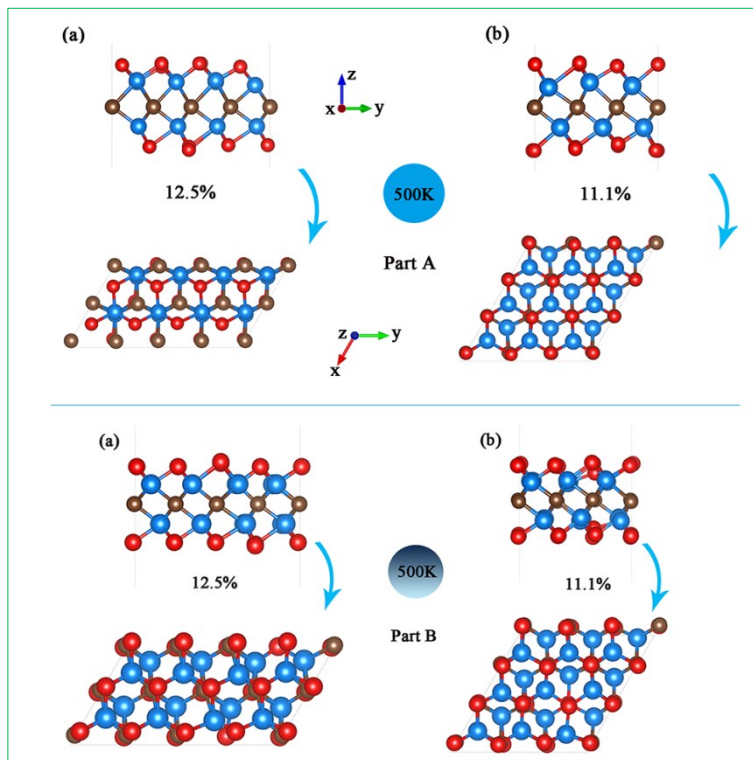


**Figure S9.** Atomic configurations of  $V_C$ - $Cr_2CO_2$  at end of *ab initio* molecular dynamics (AIMD) simulations under the temperature of 500K. The AIMD calculations were typically run for 8ps (Part A) and 4ps (Part B), with a time step of 2fs. (a) 12.5%  $V_C$ - $Cr_2CO_2$  at 500K and (b) 11.1%  $V_C$ - $Cr_2CO_2$  at 500K.